Double layer in an expanding plasma: Simultaneous upstream and downstream measurements

H. S. Byhring, C. Charles, Å. Fredriksen, and R. W. Boswell

Citation: Physics of Plasmas **15**, 102113 (2008); doi: 10.1063/1.3002396
View online: http://dx.doi.org/10.1063/1.3002396
View Table of Contents: http://scitation.aip.org/content/aip/journal/pop/15/10?ver=pdfcov
Published by the AIP Publishing

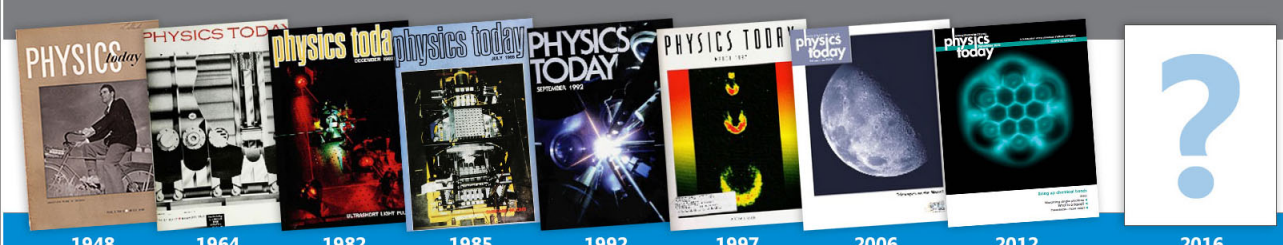

Double layer in an expanding plasma: Simultaneous upstream and downstream measurements

H. S. Byhring,[1] C. Charles,[2] Å. Fredriksen,[1] and R. W. Boswell[2]
[1]*Institute of Science and Technology, University of Tromsø, NO-9037 Tromsø, Norway*
[2]*Space Plasma, Power and Propulsion Group, Research School of Physical Sciences and Engineering, The Australian National University, Canberra, ACT 0200, Australia*

(Received 15 April 2008; accepted 29 September 2008; published online 30 October 2008)

Ion energy measurements were taken simultaneously using one retarding field energy analyzer placed at the open end of the plasma source, and one in the plasma diffusion region of an expanding low pressure argon plasma. An electric double layer was found, which is well separated from the region of high magnetic field and which is downstream of the maximum in the magnetic field gradient. An axially movable analyzer was used to determine the position of the double layer. It appears to be more closely connected to the rapid change in diameter from the source to the diffusion chamber, but still has a radial dimension close to that of the source diameter. These results suggest that the double layer forms, not as much as a result of a magnetic nozzle, but rather as a reaction to a dramatic change in boundary conditions. Still, a magnetic field of at least a few tens of Gauss in the double layer region is necessary for its spontaneous formation. © *2008 American Institute of Physics*. [DOI: 10.1063/1.3002396]

I. INTRODUCTION

Although electric double layers have been measured in the laboratory for the past 30 years (see reviews by, e.g., Charles,[1] Hershkowitz,[2] and references therein), it is only recently that current-free double layers have been reported in expanding, weakly magnetized plasmas (e.g., Refs. 3–7). In most of the experiments it has been difficult to determine whether the double layer forms in the neck of a "magnetic nozzle," in a region of rapidly expanding magnetic field, in a region of rapidly expanding plasma flow, or as a result of a change in the boundary conditions, e.g., a change in diameter of the vacuum vessel, or a transition from an insulated source to a grounded main chamber. In the experimental device used in this work, the region of maximum expansion in the magnetic field is well separated from the region where the plasma chamber expands. Since these types of experiments are of relevance to space plasma phenomena, such as, the aurora[8,9] and coronal funnels on the sun,[10] it is important to determine whether the double layer can only exist in an insulating plasma source that can charge up and anchor the double layer to the walls, or whether the double layer can exist beyond the confines of the plasma source region, in essence, being detached from the physical confines of the plasma source. In this paper we provide evidence that the double layer in an expanding, weakly magnetized plasma can exist several centimeters downstream of the insulating plasma source tube and that the double layer is formed close to the region where the plasma chamber expands.

II. DEVICE

The experiment was carried out in the "Njord" device (Fig. 1), which consists of a 1.2 m long vacuum chamber fitted with a spherical dome, of diameter 60 cm, at one end. A sketch of the experimental setup is shown in Fig. 1(a). A 31.3 cm long helicon plasma source is fitted coaxially on the dome. The plasma source consists of a 30.5 cm long Pyrex tube with inner diameter of 13.7 cm, and a grounded end plate, placed inside a 31.3 cm long grounded, metal cylinder. Between the source and the grounded dome there is a junction, consisting of a grounded cylindrical port opening, of length 6 cm and inner diameter of 20 cm, termed the "source tube extension" in the following sections. The source is adopted from the one used in the "Chi-Kung" device at the Australian National University,[3,11] and has a double-saddle rf-antenna fed with 13.56 MHz cw from a Henry Radio 8 K ultra rf amplifier and fitted with a pi-network tuning system with vacuum capacitors. The rf power output used for plasma breakdown in this experiment was held in the range 300–600 W.

Two 9.5 cm wide solenoids are fitted outside the antenna around the Pyrex tube, one centered at 1.8 cm and the other at 23.3 cm from the closed end of the Pyrex tube, which is chosen as our point of reference ($z=0$). The solenoids produce an axial magnetic field of up to 110 G in the present configuration, with a maximum current of 5 A in coil number one (at $z=1.8$ cm) and 7 A in coil number two (at $z=23.3$ cm). Three examples of the on-axis magnetic field used in this experiment are shown in Fig. 1(b), together with the corresponding gradient in the z-direction [Fig. 1(c)]. For all three current configurations in Fig. 1, the ions are weakly magnetized, with a Larmor radius which is larger than twice the source tube radius. The base pressure of the vacuum vessel in the present experimental configuration was about 0.02 mTorr. Argon gas was inserted in the end plate at a flow rate between 1.7 sccm and 21.4 sccm, providing a working gas pressure between 0.1 mTorr and 1.9 mTorr in the vacuum vessel.

To obtain information on the ion energy distributions, two retarding-field energy analyzers (RFEAs) were inserted

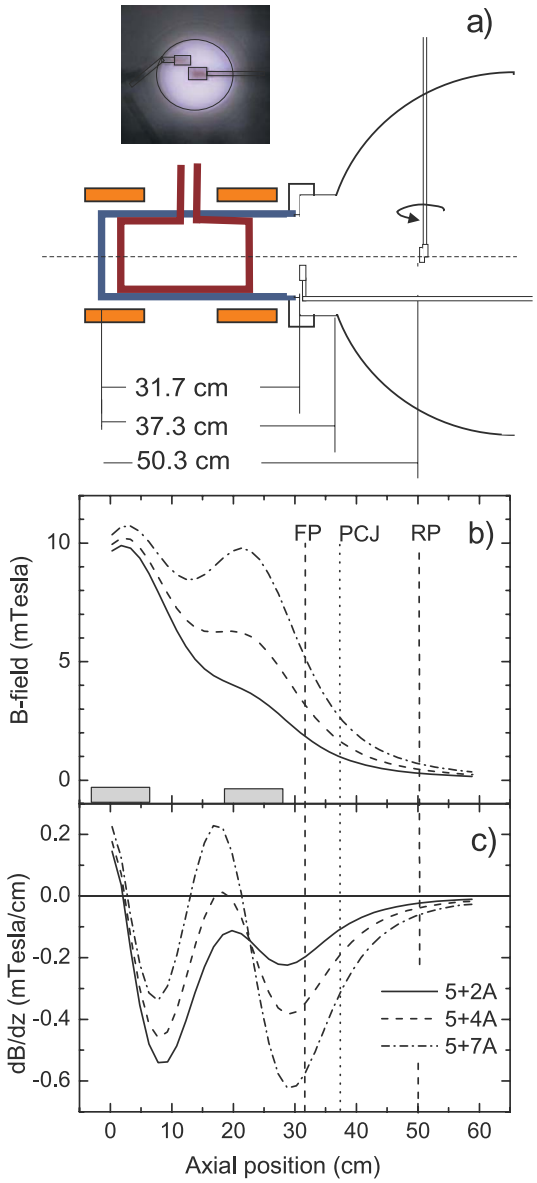

FIG. 1. (Color online) Schematic of the Njord device (a), with analyzer positions indicated. Also shown is the on-axis magnetic field (b) and the magnetic field gradient, dB_z/dz (c). The position of the maximum in the magnetic field gradient for the three cases is 28.4 cm (5+2A), 28.9 cm (5+4A), and 29.6 cm (5+7A). The locations of the ANU RFEA (Front Probe, FP), the UiT RFEA (Rear Probe, RP) and the source-chamber junction (Plasma Chamber Junction, PCJ) are indicated in panels (b) and (c) by vertical lines.

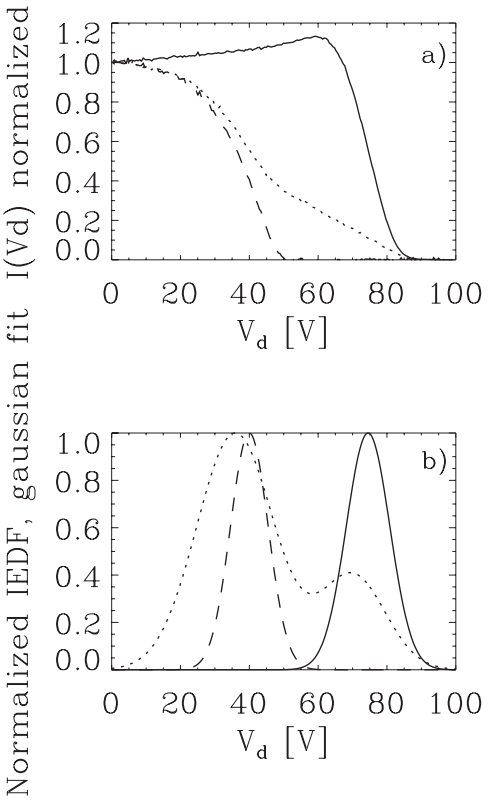

FIG. 2. (a) Current-voltage characteristics and (b) corresponding normalized IEDFs obtained upstream with the ANU RFEA (solid line) and downstream with the UiT RFEA. Dotted line: I_{axial} (i.e., facing the source); dashed line: I_{radial} [i.e., facing the chamber wall at 0.18 mTorr, with a forward rf power of 540 W, and a source magnetic field as shown in Fig. 1(b)] (5+7A).

downstream from the Pyrex tube. One, built at the Australian National University (ANU),[12] was placed with its front orifice plate normal to the z-axis and facing the tube at the fixed position $z=31.7$ cm, i.e., 0.4 cm from the edge of the plasma source tube. In the radial direction, it was placed 3.5 cm outward from the z-axis about 60° above the center plane [see Fig. 1(a)]. The other RFEA, built at the University of Tromsø (UiT), was inserted through a radial port centered at $z=50.3$ cm. This analyzer could be moved radially as well as rotated 360° around its own axis [see Fig. 1(a)]. When this analyzer was centered, the two analyzers, viewed from the downstream direction, did not overlap, as seen in the photo in Fig. 1(a). It is worth noting that both RFEAs are positioned downstream of the maximum gradient of the magnetic field [Fig. 1(c)] for all the different field configurations of the experiment. In a later setup, an axially moving analyzer was inserted to obtain details of the position of the double layer.

The ANU and UiT RFEAs had orifice diameters of 2 mm and 1 mm, respectively, and were both constructed with a mesh across the orifice in the grounded front end plate. Their electron repeller grids were biased at −85 V, the discriminator grid had variable bias from −100 V to +100 V, the secondary repeller grids were biased at −18 V, and collectors at −10 V. The distance between each grid was 0.5 mm, resulting in an overall distance between the front end grid and the collector of 2.0 mm. The axially moving analyzer had similar parameters, but a ceramic housing with a floating orifice plate. The discriminator was biased in 400 steps per scan. At each step the collector current, measured over a 10 kΩ resistor, was digitized into 300 samples which were then averaged into one single value, and written to file for further processing.

III. RESULTS

Figure 2(a) shows the normalized collected current versus discriminator voltage for the two analyzers, located at $z=31.7$ cm (ANU RFEA) and $z=50.3$ cm [UiT RFEA, see also Fig. 1(a)]. The current-voltage characteristics were obtained in an argon plasma produced at a forward rf power of 540 W (reflected power less than 20 W), with a pressure of

0.18 mTorr and a magnetic field of about 90 Gauss in the source [dashed-dotted line in Fig 1(b)]. The ANU analyzer (solid line) measures the ion current axially, with the entrance facing the source. The UiT analyzer measures the current first axially (dotted line), before it is rotated 90° to face the chamber wall (dashed line). Figure 2(b) shows the corresponding normalized ion energy distribution functions (IEDF), obtained by making Gaussian fits to the differentiated current versus voltage characteristics using a deconvolution method detailed previously by Ref. 11.

The ANU analyzer measures a single ion energy distribution, with the maximum located at the local plasma potential ($V_d = V_{p_{up}} \sim 75$ V). When oriented axially (facing the source) the UiT analyzer measures an IEDF with two peaks, one corresponding to the background ion population at the local plasma potential ($V_d = V_{p_{down}} \sim 36$ V), and one corresponding to the ion beam ($V_d = V_{beam} \sim 70$ V). When oriented radially, i.e., facing the chamber wall, the UiT analyzer measures a single distribution, peaking at $V_d = V_p \sim 40$ V. These results indicate that the double layer is positioned downstream of the ANU RFEA.

As we can see from Fig. 1(c) (dashed-dotted line), the maximum in the magnetic field gradient occurs close to the exit of the source tube, at $z = 29.6$ cm, i.e., 2.1 cm upstream of the first analyzer. The magnetic field strength in the region downstream of the source tube exit, is less than half of the maximum field strength, which occurs well inside the source tube. Thus, the double layer is positioned downstream of both the region of high magnetic field and of the maximum in the magnetic field gradient.

The double layer potential drop, Φ_{DL}, is assumed to be equal to $V_{beam} - V_p = 34$ V. This is an estimate, and the actual potential drop of the double layer might be smaller, since the plasma potential is seen to decrease somewhat in the region downstream of the double layer.

The ratio between the density of the beam ion population, n_{beam}, and the density of the background ion population, n_s, can be estimated as[11]

$$\frac{n_{beam}}{n_s} = \left[\frac{I_{axial}(V_{beam})}{I_{axial}(0) - I_{axial}(V_{beam})}\right]\frac{c_s}{v_{beam}} \sim 0.075 \pm 0.008, \quad (1)$$

where $I_{axial}(0)$ and $I_{axial}(V_{beam})$ is the collected current in the axial direction at zero discriminator voltage, and at $V_d = V_{beam}$, respectively. When the current-voltage characteristics are obtained, the sweep voltage varies between −100 and 100 V. Theoretically, the current collected for negative discriminator voltages should be equal to the current collected at $V_d = 0$, however, in reality it may vary by up to 10%–20%, probably as a result of secondary electron sputtering. The estimate above is an average value, i.e.,

$$\overline{\frac{n_{beam}}{n_s}} = \frac{1}{N}\sum_{V_d=-100V}^{V_d=0V}\left[\frac{I_{axial}(V_{beam})}{I_{axial}(V_d) - I_{axial}(V_{beam})}\right]\frac{c_s}{v_{beam}} = 0.075, \quad (2)$$

where $N = 200$ is the number of steps in the sweep voltage between −100 and 0 V. The uncertainty refers to the standard deviation of n_{beam}/n_s, owing to the variability of the collected current for negative bias voltages. Using both the radial and the axial measurement of the current, we can also estimate the density of the beam ion population as[11]

$$\frac{n_{beam}}{n_s} = \left[\frac{I_{axial}(0)}{I_{radial}(0)} - 1\right]\frac{c_s}{v_{beam}} \sim 0.07 \pm 0.012, \quad (3)$$

where $I_{radial}(0)$ is the collected current in the radial direction at zero discriminator voltage. The two estimates are in relatively good accordance. The beam density found here is about half of the value found by Ref. 11 at a pressure of 0.35 mTorr, i.e., about two times the pressure for which our data was obtained. For a pressure of 0.35 mTorr, we find a beam density of only about $0.02 n_s$, i.e., much lower than that of Ref. 11. As will be seen later, the distance from the double layer to the analyzer is comparable to that in the study of Ref. 11, about 12 cm. The magnetic field used in the study of Ref. 11 is more than twice the strength of the maximum magnetic field that can be produced in Njord, and as we will show later, the beam density decreases with decreasing magnetic field strength. It is therefore reasonable to believe that the large difference in relative beam density could be, at least partially, a result of the lower magnetic field in Njord. In addition, the expansion from the source to the diffusion chamber in the Njord device is much larger than in the Chi-Kung device, which might also have some effect on the relative beam density.

The results in Fig. 2 shows that the double layer is formed downstream of the ANU RFEA. The exact location of the double layer with respect to the expanding chamber is of interest as an indication of the relative importance of the expanding magnetic field and the expanding chamber in the formation of the double layer. To further investigate the position of the double layer, a third RFEA (hereafter termed axial RFEA) was placed on an axially movable arm. The setup for the axial RFEA is shown in Fig. 3. The axial RFEA is different from the UiT RFEA and the ANU RFEA in that it floats with respect to the plasma. Thus, the axial RFEA is expected to cause less disturbance to the plasma than the grounded analyzers. As will be seen later, the results from the floating analyzer are very similar to those of the grounded ones, which imply that the disturbance to the plasma caused by grounding the analyzer is not significant with respect to the measured potentials. In addition, we might see a change in the width of the IEDF in the floating RFEA compared to the grounded ones, resulting from the fact that the rf sheath in front of the floating analyzer will be different from that of the grounded ones. However, we are only interested in obtaining the plasma and beam potentials, and the width of the IEDF is not important in this context. The axial RFEA was inserted with the orifice hole located about 1 cm above the z-axis ["pos 1" in Fig. 3(b)], at $z = 51.1$ cm, and facing the source. It was then moved axially 20 cm in the direction of the source in steps of 2 cm. The axial scan was repeated with the analyzer located in the center plane of the source, at $r = R_{source} - 1.8$ cm ["pos 2" in Fig. 3(b)].

The results for the first axial scan (analyzer in "pos 1"),

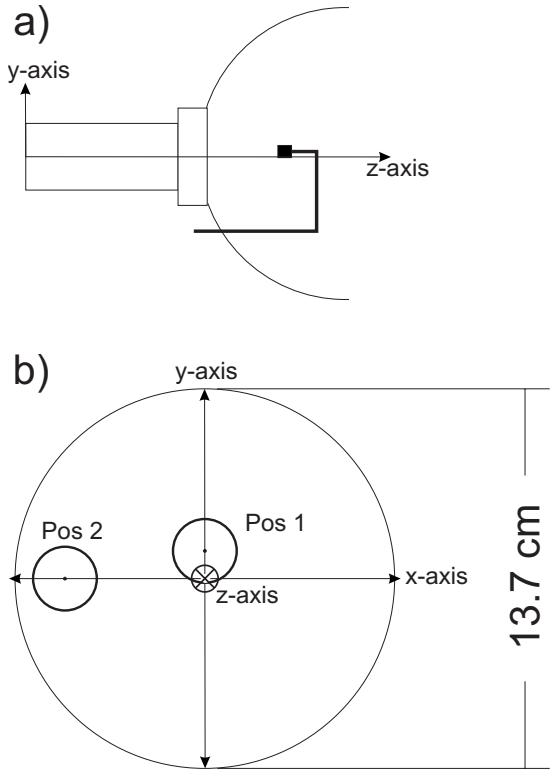

FIG. 3. "Side view" of Njord showing the axial analyzer in the initial position (a) at $z=51.1$ cm, and analyzer positions as viewed from the source tube looking downstream (b) toward the expanding main chamber.

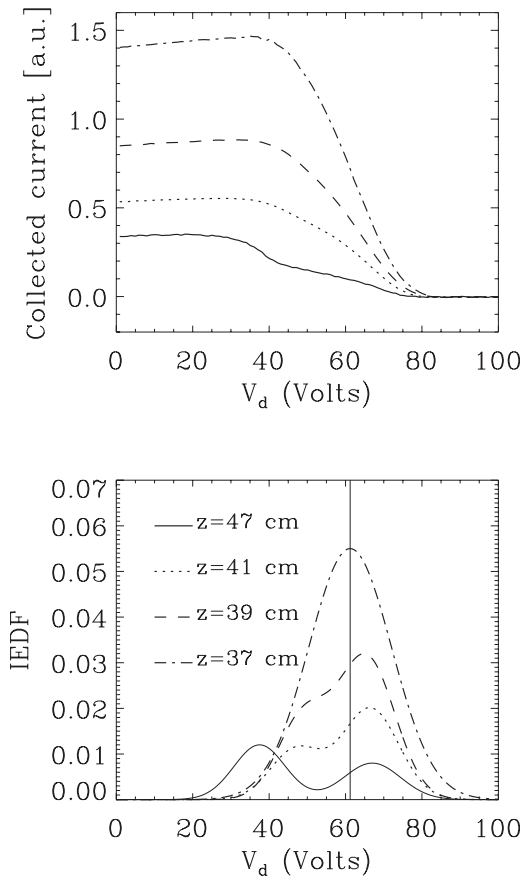

FIG. 4. Collected current vs discriminator voltage (upper panel) and Gaussian fits to the derivatives of the current-voltage characteristics vs discriminator voltage (lower panel) for four different axial positions.

taken at a pressure of 0.18 mTorr, can be seen in Fig. 4, where we have plotted the original I-V curves (upper panel) together with Gaussian fits to the derivatives of the current-voltage characteristics (lower panel) as function of discriminator voltage. For the Gaussian fits, the peak fitting module in OriginPro 8™ was used. At $z=37$ cm a single-peak maximum was obtained at 54.46 ± 0.18 V, with a width of 25.4 ± 0.4 V. At $z=47$ cm the beam maximum was located at 57.9 ± 0.9 V, with a width of 20 ± 2 V, and the background distribution had a maximum at 31.2 ± 0.3 V with a width of 10.7 ± 0.7 V.

The beam is first seen at about $z=39$ cm, which is just downstream of the exit of the source tube extension. We therefore conclude that the ions are accelerated into a beam between $z=37$ cm and $z=39$ cm, i.e., in the region where the plasma chamber starts to expand. The beam potential stays between 65–67 V, which is 3–5 V lower than the beam potential for the same pressure in Fig. 6. Generally it has proved difficult to exactly reproduce the observed beam and plasma potentials with the UiT and the axial RFEA. The curve-fitting process is sensitive to noise, and the potentials derived in the analysis of the data should be considered rough estimates. As the analyzer moves toward the source, the peak in the IEDF corresponding to the background ion population moves towards higher potentials. One unexpected feature in this plot is that the upstream plasma potential seems to be lower than the beam potential in the region immediately downstream of the double layer. This could be explained by the fact that the collision cross section is energy dependent.[13] The high-energy ions thus preserve their directional energy over longer distances, while the low-energy ions are lost from the beam, leading to an increase in the average energy of the beam.

For the second axial scan, near the edge of the source tube (analyzer in "pos 2"), the results were similar. Here, the beam is also visible at $z=37$ cm, meaning that the double layer is positioned a bit further inside the source tube extension, between $z=35-37$ cm. The position of the double layer has not been investigated further, and with the presently available diagnostics, it is not possible to deduce whether the double layer is bounded radially by the insulating glass source tube or the grounded source tube extension. To answer this question, a complete three-dimensional mapping of the plasma potential in the source and source tube extension must be carried out. However, it is important to note that for the axial RFEA, and especially in the region close to the exit of the source tube, the peak in the IEDF corresponding to the background ion population does not necessarily occur at the true plasma potential, because the plasma is flowing along the line of sight of the analyzer, a problem which was also pointed out by Charles.[1] Detailed measurements of the plasma potential inside the source therefore requires the construction of an axially movable analyzer which faces the plasma chamber wall, and such an investigation is therefore outside the scope of this paper.

Figure 5 shows the variation with pressure of (a) plasma

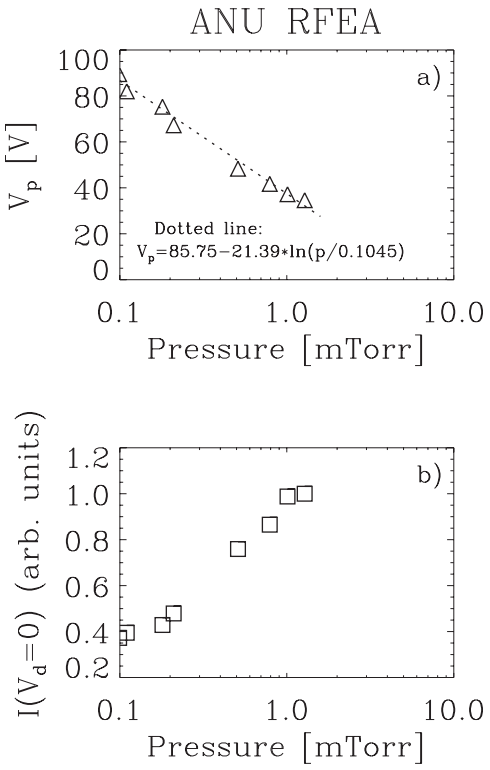

FIG. 5. (a) Plasma potential and (b) total ion current obtained upstream with the ANU RFEA (z=31.7 cm) plotted vs pressure.

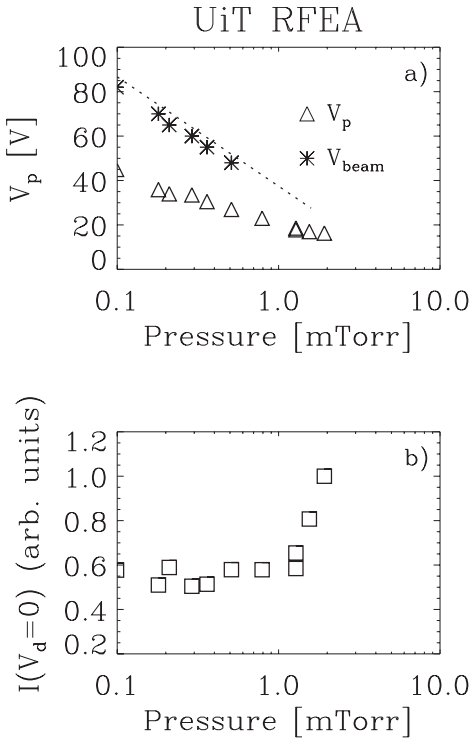

FIG. 6. (a) Plasma potential and beam potential and (b) ion saturation current obtained downstream with the UiT RFEA plotted vs pressure. The dotted line corresponds to the exponential fit to the plasma potential measured by the ANU RFEA upstream, from Fig 5(a).

potential and (b) collected current at zero discriminator voltage, measured upstream of the double layer. The plasma potential decreases exponentially with pressure, and the collected current increases almost exponentially with pressure. An exponential fit of the Vp upstream is shown by a dotted line in Fig. 5(a). In the downstream region (Fig. 6), the plasma potential also decreases exponentially as the pressure is increased, but not as fast as in the upstream region. The beam potential in the downstream region decreases more rapidly, with the result that the double layer potential fall decreases with increasing pressure, as expected from similar experiments (e.g., Refs. 3, 5, 7, 14, and 15). The exponential fit of Vp upstream [dotted line in Fig. 5(a)] is also shown on Fig. 6(a). The results in Fig. 6 also show that above 0.5 mTorr the ion beam is no longer visible at the position of the UiT analyzer. The collected current [Fig. 6(b)] varies little with pressure below 1 mTorr in the downstream region. Above this pressure, the collected current increases rapidly.

As can be seen in Fig. 6, the double layer in Njord can be sustained for pressures up to 0.5 mTorr, whereas in Chi-Kung the double layer can be observed for pressures as high as 1.13 mTorr. On the other hand, it seems that the double layer in Njord can be more easily sustained for low pressures, with a minimum pressure of about 0.1 mTorr versus 0.2 mTorr for Chi-Kung. This is probably a result of the larger diffusion chamber in Njord, and is consistent with the results of Ref. 7, who found a double layer in the large volume helicon diffusion system WOMBAT (waves of magnetized beams and turbulence) for pressures in the range 0.09–0.3 mTorr.

The collected current in the axial direction, at the beam potential, can be expressed as

$$I_{\text{axial}}(V_{\text{beam}}) = eAT^4 n_{\text{beam}} v_{\text{beam}}, \tag{4}$$

where e is the elementary charge, A is the area of the analyzer aperture, and T is the grid transmission factor (the analyzer has four grids). With the average velocity of the beam ions equal to

$$v_{\text{beam}} = \sqrt{\frac{2e(V_{\text{beam}} - V_p)}{m_i}}, \tag{5}$$

it then follows that if $\Phi_{\text{DL}} = V_{\text{beam}} - V_p$ is constant for varying r, the axial current at the beam potential is proportional to the beam density, n_{beam}. By inspection of the current-voltage characteristics, and their corresponding IEDFs, it was found that the double layer potential drop is constant between r =0 and r=11 cm. The beam density is plotted versus radial position of the analyzer in Fig. 7, for a pressure of 0.11 mTorr. The beam density decreases, from a maximum at r=0 cm, to about 14% of the maximum value at r =11 cm.

To investigate how the properties of the double layer depend on the magnetic field strength, the current in the second source coil (see Fig. 1) was reduced in steps of 1 A until the ion beam was no longer detectable at the UiT RFEA. In Fig. 8 we have shown the IEDFs obtained with the current configurations shown in Fig. 1. As the current in the second coil is reduced, the plasma potential and the beam density decreases. For currents of 2 A or lower in the second coil, corresponding to a magnetic field in the upstream region

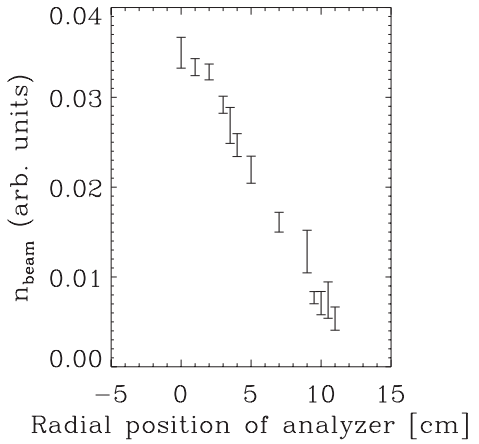

FIG. 7. Beam density plotted vs radial distance for a pressure of 0.11 mTorr.

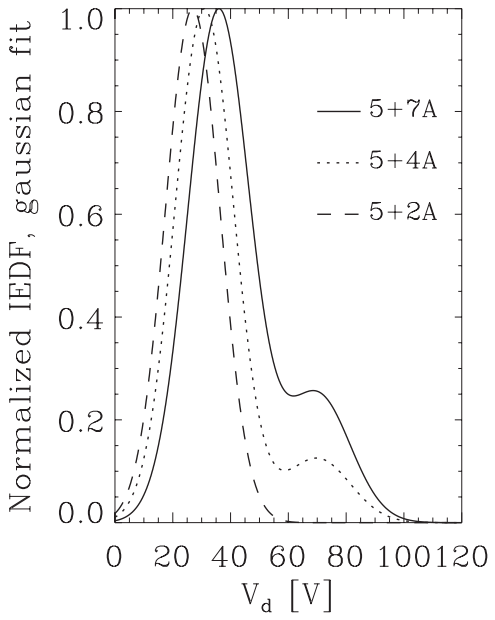

FIG. 8. Normalized IEDFs for three different source coil current configurations, the corresponding on-axis magnetic fields are shown in Fig. 1.

$(20 \leqslant z \leqslant 30$ cm) of about 30 Gauss, the measured current-voltage characteristics can be adequately fitted to one Gaussian, meaning that the ion beam, and the double layer, is lost. This result is consistent with previous studies of the exhaust magnetic field on the DL formation and properties in argon[16] and xenon.[17] The magnetic field strength in the region where the double layer is formed, i.e., downstream of the ANU RFEA at $z=31.7$ cm, is less than half the value of the magnetic field inside the source tube. Thus, the double layer is well separated from the region of high magnetic field. Under the assumption that the double layer is positioned between $z=37-39$ cm, as discussed in connection with Fig. 4, we find that the distance from the closest maximum in the magnetic field gradient to the double layer is between 7 cm and 10 cm.

IV. SUMMARY

An ion beam, created by an electric double layer, has been observed in the inductively coupled plasma of the Njord device using two retarding field energy analyzers to obtain simultaneous measurements of the upstream and downstream ion energy distributions. One analyzer was placed immediately outside the glass source tube and the other was placed in the plasma diffusion region of the expanding, low pressure argon plasma.

Measurements with an axially movable analyzer show that the double layer is formed close to the junction between the source tube extension and the expanding chamber (i.e., 6 cm downstream of the exit of the insulated source tube) for $r=0$ cm and $r=R_{source}-1.8$ cm. In addition, the double layer forms well downstream of both the region of high magnetic field, and of the maximum in the magnetic field gradient. This indicates that the double layer forms, not as a result of the expanding magnetic field, but as a result of the rapid expansion of the plasma chamber. Still, a magnetic field of at least a few tens of Gauss in the double layer region is necessary for its spontaneous formation. Regarding the radial extent, and geometry, of the double layer, our data are not conclusive, and a more precise determination of the location and radial extent of the double layer should be carried out. The double layer and beam properties are consistent with the results of similar studies.[1]

[1] C. Charles, Plasma Sources Sci. Technol. **16**, R1 (2007).
[2] N. Hershkowitz, Space Sci. Rev. **41**, 351 (1989).
[3] C. Charles and R. Boswell, Appl. Phys. Lett. **82**, 1356 (2003).
[4] S. A. Cohen, N. S. Siefert, S. Stange, R. F. Boivin, E. E. Scime, and F. M. Levinton, Phys. Plasmas **10**, 2593 (2003).
[5] N. Plihon, P. Chabert, and C. S. Corr, Phys. Plasmas **14**, 013506 (2007).
[6] X. Sun, A. M. Keesee, C. Biloiu, E. E. Scime, A. Meige, C. Charles, and R. W. Boswell, Phys. Rev. Lett. **95**, 025004 (2005).
[7] O. Sutherland, C. Charles, N. Plihon, and R. W. Boswell, Phys. Rev. Lett. **95**, 205002 (2005).
[8] R. E. Ergun, Y.-J. Su, L. Andersson, C. W. Carlson, J. P. McFadden, F. S. Mozer, D. L. Newman, M. V. Goldman, and R. J. Strangeway, Phys. Rev. Lett. **87**, 045003 (2001).
[9] R. E. Ergun, L. Andersson, D. Main, Y.-J. Su, D. L. Newman, M. V. Goldman, C. W. Carlson, J. P. McFadden, and F. S. Mozer, Phys. Plasmas **9**, 3695 (2002).
[10] R. W. Boswell, E. Marsch, and C. Charles, Astrophys. J. Lett. **640**, L199 (2006).
[11] C. Charles and R. W. Boswell, Phys. Plasmas **11**, 1706 (2004).
[12] C. Charles, A. W. Degeling, T. E. Sheridan, J. H. Harris, M. A. Lieberman, and R. W. Boswell, Phys. Plasmas **7**, 5232 (2000).
[13] A. V. Phelps, J. Appl. Phys. **76**, 747 (1994).
[14] M. A. Lieberman and C. Charles, Phys. Rev. Lett. **97**, 045003 (2006).
[15] C. Charles, Phys. Plasmas **12**, 044508 (2005).
[16] C. Charles and R. W. Boswell, Appl. Phys. Lett. **91**, 201505 (2007).
[17] C. Charles and R. W. Boswell, "Effect of exhaust magnetic field in helicon double-laye thruster operating in xenon," IEEE Trans. Plasma Sci. (unpublished).